Holographic Control of Electric Field Distribution for Mobile Communication

Masahiro Daibo† Hiroshi Okazaki‡ and Yasunori Suzuki‡

†Faculty of Science and Engineering, Iwate University 4 - 3 - 5 Ueda, Morioka, Iwate, 020-8551 Japan

‡NTT DOCOMO, INC., Sanno Park Tower 11 - 1, Nagata-cho 2-chome, Chiyoda-ku, Tokyo 100-6150 Japan

E-mail: †daibo@iwate-u.ac.jp, ‡{okazakih, yasunori.suzuki.ws}@nttdocomo.com

Abstract In order to make effective use of radio wave resources and to prevent interference, it is important to increase the electric field strength at the place where the user is present and to decrease the electric field strength where the user is not present. To investigate the feasibility of this requirement, we performed simulations with computer generated hologram. When the microwave was emitted from each antenna according with amplitude of the hologram, the electric field distribution in the plane where the users were located was reconstructed successfully. We demonstrate that by installing a sufficient number of antennas, depending on the distance, the desired field distribution can be obtained.

Keyword Computer Generate Hologram, Microwave Holography, Mobile Communication

1. INTRODUCTION

In mobile communication, there is an increasing demand for communication capacity. Multiplexing and carrier frequency increase are important to meet the demand. Recently, attention is being paid to OAM (Orbital Angular Momentum) [1] as multiplexing, and this technique can be said to be a method for preventing mutual interference between a large number of channels.

On the other hand, when the carrier frequency is increased, diffraction is reduced, absorption is increased, then higher carrier is less likely to reach the destination. As a result, the number of antennas has to be increased in the next generation system.

If an increase in the number of antennas cannot be avoided, it may be better to control the wavefront by holography [2] even in the microwaves. Although it is static, experiment has been conducted to control the wave front of an electromagnetic wave by holography in the sub-terahertz region.[3] Holography can coexist with OAM and complement each other, because electromagnetic waves with different polarizations do not interfere. OAM and holography can be used as next generation's physical layers.

Microwave holography was applied for dielectric targets imaging [4] and cancer imaging [5], but as far as I know, there have been no reports of aggressive use in mobile communications.

This paper is to estimate whether holography can be used with the wavelength of microwave and the dimension of human living space, by anticipating wavelength shortening and the installation of a large number of antennas in future. Specifically, the purpose of this paper is to generate an electric field with an arbitrary spatial distribution at the user's location.

2. COMPUTER GENERATED HOLOGRAPHY

First, we assume two planes. One is a plane on which users (for example, mobile phones) are present, and the other is a plane on which antennas are installed in an array. A virtual point sources generating microwave with unit amplitude are arranged at all sampling points on the user plane.

Since the distance between each sampling point on the two planes can be determined geometrically, the amplitude and phase of the arriving microwave antennas were pre-computed.

The electric field ϕ_i when the microwave of wavelength λ emitted with an amplitude E_j from the point source at the coordinate index j of the user plane reaches at the coordinate index i of the antenna array plane with the distance r_{ij} is obtained as

$$\phi_i = \sum_{j=0}^{N} \frac{E_j}{r_{ij}} \cos\left(\frac{2\pi}{\lambda} r_{ij} + \theta_j\right). \quad (1)$$

Here, the relative initial phase θ_j was set randomly. We did not take into account the polarization and simplified the wavefront as a spherical wave emitted from a point source.

The element of hologram matrix is calculated by (1) where the number of sampling points on the user plane is N. The index of the antenna arrays is i and the total number of antennas is M.

The calculation of the hologram matrix $\boldsymbol{\Phi}$ has a large amount of calculation because there are $N \times M$ combinations. However, once $\boldsymbol{\Phi}$ has been calculated, the hologram vector $\boldsymbol{h}$ can be obtained from the next time by multiplying the hologram matrix $\boldsymbol{\Phi}$ and the electric field distribution vector $\boldsymbol{b}$ on the desired user plane, as expressed

$$\boldsymbol{h} = \boldsymbol{\Phi b}. \quad (2)$$

The electric field distribution on the user plane is originally a two-dimensional image, but the coordinate index is unfolded and converted into a vector $\boldsymbol{b}$ for convenience of multiplication with the hologram matrix $\boldsymbol{\Phi}$. The hologram image is also unfolded into a vector $\boldsymbol{h}$ as well as $\boldsymbol{b}$.

Fig. 1 shows an example of the base hologram images. These images were created by folding the first four row vectors of the hologram matrix $\boldsymbol{\Phi}$. As a virtual object on the user plane, consider a group of point sources consisting of 128 × 128 pixels with uniform electric field amplitude. These figures show the electric field distribution on the antenna array plane at a distance z apart from the user plane when a spherical wave is emitted from a point source on the user plane. Fig. 1 (a) and (b) differ in distance z.

Although it may be difficult to recognize from this figure, the center of the Fresnel pattern is shifted by one pixel to the right and originates from four different point light sources. Since the initial phase was randomly changed, the central brightness of circles is also random. Here, a plane wave parallel to the antenna array plane was assumed as a reference wavefront to be a phase reference.

The interpretation of Fig.1 is as follows. If antennas are installed at every pixel of this hologram image and the antennas emit a continuous wave with an electric field amplitude proportional to the brightness of each pixel of hologram, the microwave is focused on a specific point in the space at a distance z.

It should be noted here that when all the antennas are driven simultaneously, the arrival time differs by one period per interference fringe of the black-and-white pair even though the phase is the same at the arrival location. Therefore, in the case of the modulated wave, it is necessary to wait until all of the signal arrives from the antennas. Alternatively, since the delay time can be known in advance, by radiating from the far antenna to the near antenna in order at an appropriate timing, it is possible to simultaneously focus on the certain point at all.

Since the sampling interval of the antenna array was set to 0.1 m, aliasing in the spatial domain occurs when the interval of the interference fringes is shorter than 0.2 m. The upper left in Fig. 1 (b) is a dominant Fresnel pattern, but the other Fresnel patterns are generated by aliasing. If the hologram is regarded as a simple two-dimensional stripe like pattern, the area of aliasing is meaningless, but since the hologram records three-dimensional information, the information is also recorded in the area of aliasing.

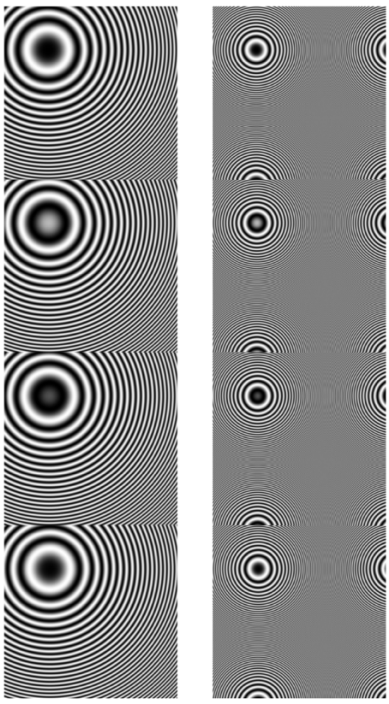

(a) (b)

Fig.1. Image of base hologram. (a) z = 1000 m. (b) z = 200m.

3. SIMULATION RESULT

The point sources were arranged to be in the shape of the letter “R” as target field distribution. The amplitude of the point source is binary. The parameters used for this simulation are as follows. The number of sampling user plane N = 128 × 128, the number of antenna arrays is M = 256 × 256, user plane sampling interval S_u = 0.1 m, antenna array interval S_a = 0.1 m, wavelength λ = 0.01 m (f = 30 GHz). The distance between user plane and antenna array plane z was varied in the range of 100 m to 1000 m. M was also varied in the range of 32 × 32 to 256 × 256, interlocking with it, S_a was inversely proportional to M.

The hologram recorded the letter “R” is shown in Fig. 2. When the distance z is large, the spatial frequency of the hologram is low because the curvature of the spherical wave is large. That is, when z is large, it means that the distance between the antennas can be increased. On the other hand, when z is small, the spatial frequency of the hologram is high, and aliasing occurs in the off-axis region where the antenna array spacing does not satisfy the Nyquist condition. The same pattern appears repeatedly as shown in Fig. 2 (a).

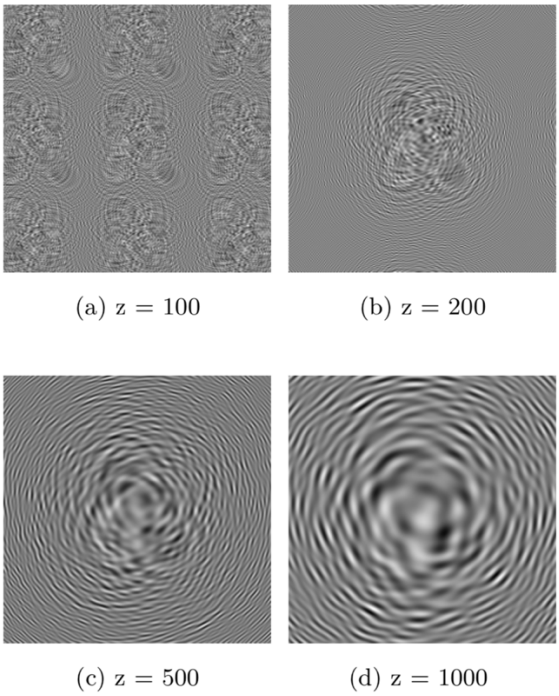

Fig.2. Hologram images. The number of hologram pixels is 256 x 256. (a) the distance between the user plane and antenna array plan, *z* is 100 m, (b) 200 m, (c) 500 m, (d) 1000 m.

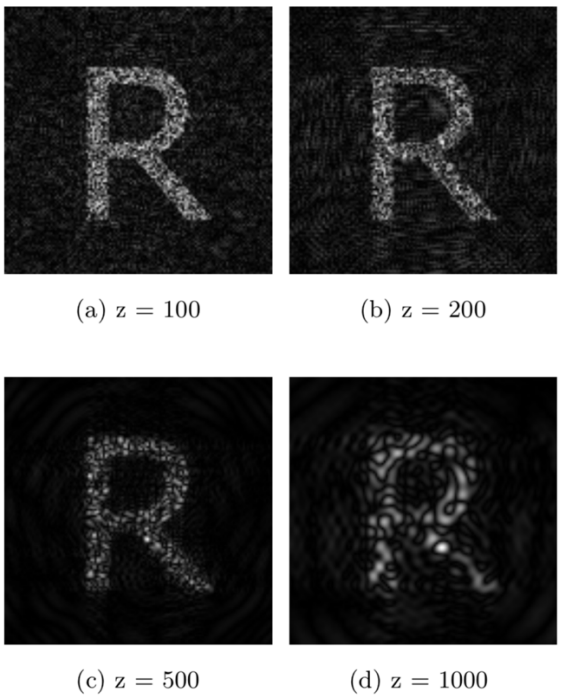

Fig.3. Reconstructed electric field distribution. The number of hologram pixels M = 256 x 256. (a) the distance between the user plane and antenna array plan, *z* is 100 m, (b) 200 m, (c) 500 m, (d) 1000 m.

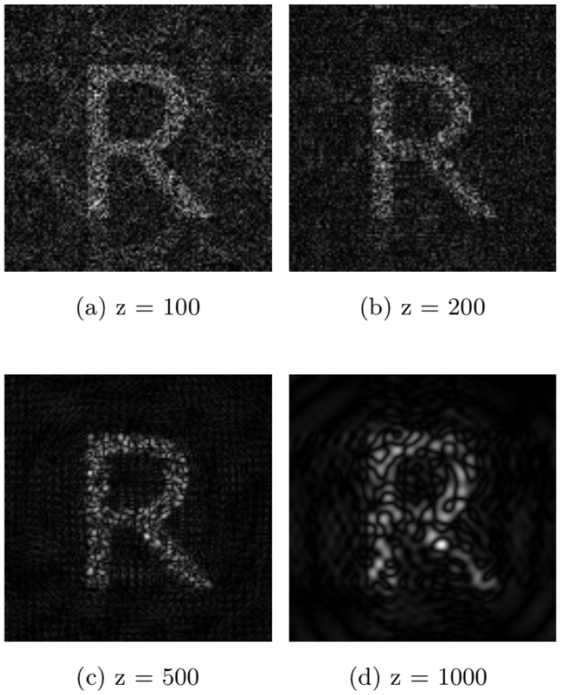

Fig.4. Reconstructed electric field distribution. The number of hologram pixels M = 128 x 128. (a) the distance between the user plane and antenna array plan, *z* is 100 m, (b) 200 m, (c) 500 m, (d) 1000 m.

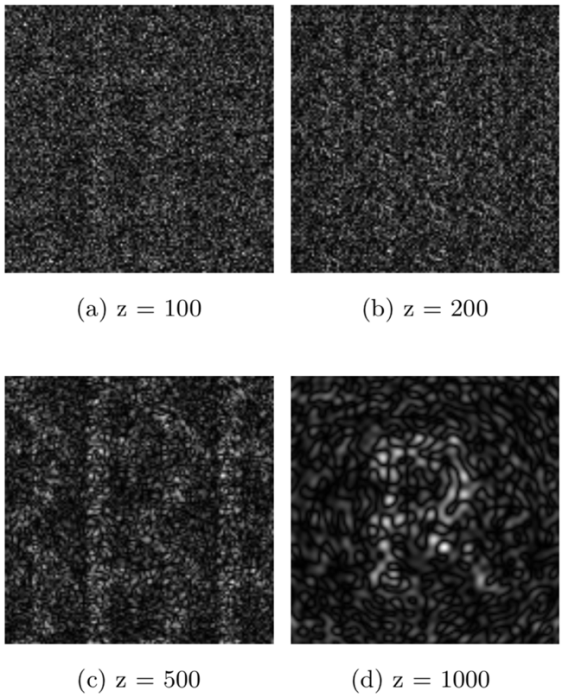

Fig.5. Reconstructed electric field distribution. The number of hologram pixels M = 32 x 32. (a) the distance between the user plane and antenna array plan, *z* is 100 m, (b) 200 m, (c) 500 m, (d) 1000 m.

The simulation results of the electric field distribution on the user plane when the parameter *M* is changed is shown in Fig. 2 – Fig. 5. The smaller the distance *z*, the higher the lateral resolution and the sharper the reconstructed image was obtained, but when *z* was too small, multiple images appeared due to aliasing. The aliasing appeared notably when *M* was small, e.g. Fig 4 (a), Fig 5 (a)-(c), because the antenna array intervals was large. Interestingly, although aliasing occured in Fig. 2 (a), sharper electric field distribution was reconstructed in Fig. 3 (a) than in Fig. 3 (b) in which no aliasing occured. Since a hologram is a three-dimensional information recorded in two dimensions, it may not necessarily be limited to two-dimensional sampling theorem, but in the real world, the sample points have a finite area and the amplitude is quantized, we should pay close attention to the aliasing.

Since a sine wave is a periodic function, a phenomenon called speckle occurs in which phases are accidentally matched or not at unintended places. In this simulation, the initial phase was set randomly, but if several sets of random are prepared, it will be possible to change the speckle pattern by switching in time division.

4. CONCLUSION

The amplitude hologram was calculated by the computer generated hologram method with the wavelength (0.01 m) of microwaves, the spatial resolution (0.1 m) in typical human living dimension, and antenna array interval of 0.1 – 0.8 m. The reconstruction simulation was also performed to confirm the distribution of electric field on the user plane.

The wavelength of the microwave is forth orders of magnitude longer than visible light, however, it has been found that the distribution of the electric field can be controlled by the hologram under the conditions that sufficient the number of elements of the antenna array and appropriate the distance between the antenna array and the users.

The hologram matrix requires very large and massive calculations, however, using our method, the matrix can be calculated in advance by modeling a virtual object consisting of uniform point electromagnetics wave sources. At the time of execution, it is possible to generate the hologram data immediately by the sum-of-products operation with the hologram matrix and the demanded field distribution map.

After emitting microwave, the redistribution of energy from areas of weak electric fields to areas of strong electric fields is performed naturally at the speed of light by the hologram.

References

[1] Fabrizio Tamburini et al, Encoding many channels on the same frequency through radio vorticity: first experimental test, New J. Phys. 14 033001(2012).

[2] Gabor, D. A new microscopic principle. Nature 161, 777–778 (1948).

[3] Mateusz Surma et al, Sub-Terahertz Computer Generated Hologram with Two Image Planes, Appl. Sci., 9, 659; doi:10.3390 (2019).

[4] Amineh, Reza K., et al. "Three-dimensional near-field microwave holography using reflected and transmitted signals." IEEE Transactions on Antennas and Propagation 59.12, 4777-4789 (2011).

[5] Nikolova, Natalia K. "Microwave imaging for breast cancer." IEEE microwave magazine 12.7, 78-94(2011).